Besseau *et al. J Wood Sci* (2020) 66:74
https://doi.org/10.1186/s10086-020-01922-y

Journal of Wood Science

ORIGINAL ARTICLE Open Access

Influence of wood anatomy on fiber orientation measurement obtained by laser scanning on five European species

Benoît Besseau*, Guillaume Pot, Robert Collet and Joffrey Viguier

Abstract

In order to obtain high production rates of sawn timber, the sawmilling industry can use laser scanning, allowing knot detection and machine strength grading. In particular, laser scanners measure grain angle using the so-called tracheid effect on wood surface where an elliptic scattering of the laser light can be observed. This paper aims to describe the light scattering obtained by a laser beam projection on wood surface and to assess the accuracy of such fiber orientation measurement on five European species. Firstly, fiber orientation measurement error was assessed by rotating samples. Secondly, the description of the scattering effect was done considering ellipse axis ratios and areas. This was studied according to several parameters such as wood surface machining, moisture content, and orthotropic planes of symmetry. Fiber orientation measurement was successfully performed on all the tested species. The measurement error was below 1.6°, except for oak longitudinal–radial (LR) plane showing an error up to 3.1°. For most of the species, the error was higher in LR plane because of the influence of medullary rays. Despite the observation of major variabilities in laser light scattering, it was possible to measure the grain angles with a good accuracy for all investigated species.

Keywords: Laser scanning, Grain angle, Tracheid effect, Fiber orientation, Hardwood, Oak

Introduction

In wood industry, the integration of scanners in production lines is more and more common because they can help to pilot automatic crosscutting and both aesthetical and mechanical grading of wood pieces. Such scanners include several types of sensors like, for example, color cameras, X-ray detectors measuring local density, but also systems based on laser dots that are able to measure locally the fiber orientation of wood timber.

The latter technology uses the fact that the light scattering is higher in the longitudinal direction of fibers than across. A circular laser dot projected perpendicularly to a wood surface takes an elliptic light shape oriented along the fibers [1, 2]. In the literature, this phenomenon is called "tracheid effect", because it was mostly developed for softwoods [1, 3]. The shape of this scattered light spot can be fitted by the equation of an ellipse with some mathematical algorithm [4–6], the orientation of the major axis giving the local fiber orientation in the plane of the considered surface. Indeed, fiber orientation is a 3D phenomenon, but tracheid effect only allows measurement of the projected fiber orientation at the scanned surface [6]. In the present paper, only the in-plane fiber orientation is studied. This angle is the main parameter studied in the literature, especially for the settings of strength grading methods [7, 8].

Other ellipse parameters, like axis ratio and area, are less often studied, while they can also characterize the light scattering effect. Nevertheless, [2] used a shape factor of the ellipses to estimate the fiber diving angle (out of the ellipse plane), but this method appears not precise enough [6]. [5] Measured the length of ellipse minor and major axes on Japanese beech (*Fagus crenata* Blume) and sugi (*Cryptomeria japonica* D.Don) on sawn and planed

*Correspondence: benoit.besseau@ensam.eu
LABOMAP, Arts et Metiers Institute of Technology, HESAM Université, 71250 Cluny, France

wood surfaces, while rotating samples. They showed that, for both species, the grain angle measurement error on the planed samples was lower than on rough-sawn samples (maximum error of 4.6° for rough-sawn sugi), which is in accordance with [9] on Douglas fir. In [5], no analysis was provided regarding the major and minor axis length for the two species and two surface machining, and only one laser dot was used [10]. Used ellipse eccentricity to detect knots [11] determined that ellipses are bigger on wet wood than on dry wood and proposed a physical model. On the same topic, [12] showed that the ellipse size increases with moisture content (MC) of beech and poplar veneers.

This literature review shows that parameters such as surface machining, MC and wood species influence ellipse shape, and thus potentially the accuracy of fiber orientation measurement. Nevertheless, only [5] suggested there is a relationship between ellipse shape and the measurement accuracy of ellipse angle. Moreover, there is no wide comparison of the tracheid effect between species, except in [13] concluding that a split laser with a wavelength of 660 nm and power of 100 mW do not provide satisfactory results on oak (*Quercus* spp. L.).

The objectives of this paper are to analyze laser light scattering and to design an accurate fiber orientation measurement at the surface of several European softwoods and hardwoods species: Douglas fir (*Pseudotsuga menziesii* Mirb. Franco), poplar (*Populus*), beech (*Fagus sylvatica*), sweet chestnut (*Castanea*) and oak (*Quercus petraea* and *Quercus robur* L). Oak species were studied in more detail. The measurement error of fiber orientation was assessed by measuring angles for several known sample rotations. The description of the scattering effect was done using axis ratios and ellipse areas. Both of these topics were studied according to several parameters such as surface machining, MC and orthotropic planes of symmetry. To the best of authors' knowledge, no paper has been published regarding this last parameter, while wood anatomy is obviously significantly different because of radial growth and rays orientation.

Material and methods

Sampling

Five wood species have been studied: sweet chestnut (*Castanea sativa*), Douglas fir (*Pseudotsuga menziesii* Mirb. Franco), poplar (*Populus*), beech (*Fagus sylvatica*) and oak (*Quercus petraea* and *Quercus robur* L).

For each species, 10 samples ($100 \times 100 \times 20$ mm^3) were selected from 5 quarter-sawn boards and 5 flat-sawn boards, in order to obtain, respectively, 5 samples with their faces in the longitudinal–radial plane (LR plane) and 5 with their faces in the longitudinal–tangential plane (LT plane) (Fig. 1). All samples were made of clear wood. Tests on sweet chestnut, Douglas fir, poplar and beech were performed on samples at room MC equilibrium (MC between 8 and 12%); their surfaces have been planned with an industrial planing machine to obtain low surface roughness.

Each of the oak samples has been studied at three different MC/surface machining states: (i) "green oak" state, just after sawing at a MC above fiber saturation point (FSP) (around 90% MC measured after weighting samples once they had dried) and a rough sawn surface; (ii) "dry oak" state, the same samples having been naturally dried being still with the rough sawn surface finish; (iii) "sanded oak" state, the dry oak samples being then sanded to be studied with a smoother surface.

In addition, 4 samples of high-density fiberboard (HDF) were chosen for their almost isotropic properties for comparison with solid wood samples.

Scanner

Fiber orientation was measured with BobiScan, a laboratory scanner developed in Arts et Métiers Cluny (France). This device is equipped with a near-infrared camera (Basler acA2000-340 km NIR, 2048×1088 pixels, 340 frames per second), recording images of the light scattering effect obtained with infra-red laser rays (wavelength of 1064 nm and power up to 1 W) with an exposure time of 1800 µs and a gain of 33. The incident laser light had an advertised diameter of 2 mm and was divided in several rays 10 mm spaced by a diffractive optic element (Fig. 2c). A software was developed to record the position of each laser dot while the board was moved in a longitudinal direction on a conveyor below the scanning system, resulting in a resolution of 1 mm in this direction.

The power of each laser dot was measured at the surface sample level with a compact USB power meter (Thorlabs' PM 16–121) for two different input powers of laser source (Table 1). Indeed, laser power was adjusted at setting 1 for all the samples except for green oak and poplar ones, ellipse major axis obtained in these cases reaching sometimes up to 10 mm, which was the distance

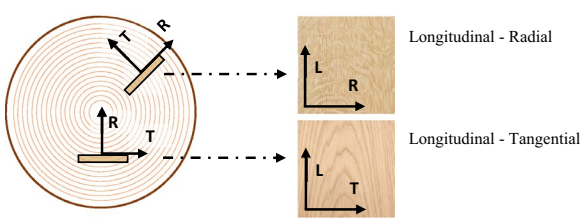

Fig. 1 Description of orthotropic planes of symmetry: example of oak samples

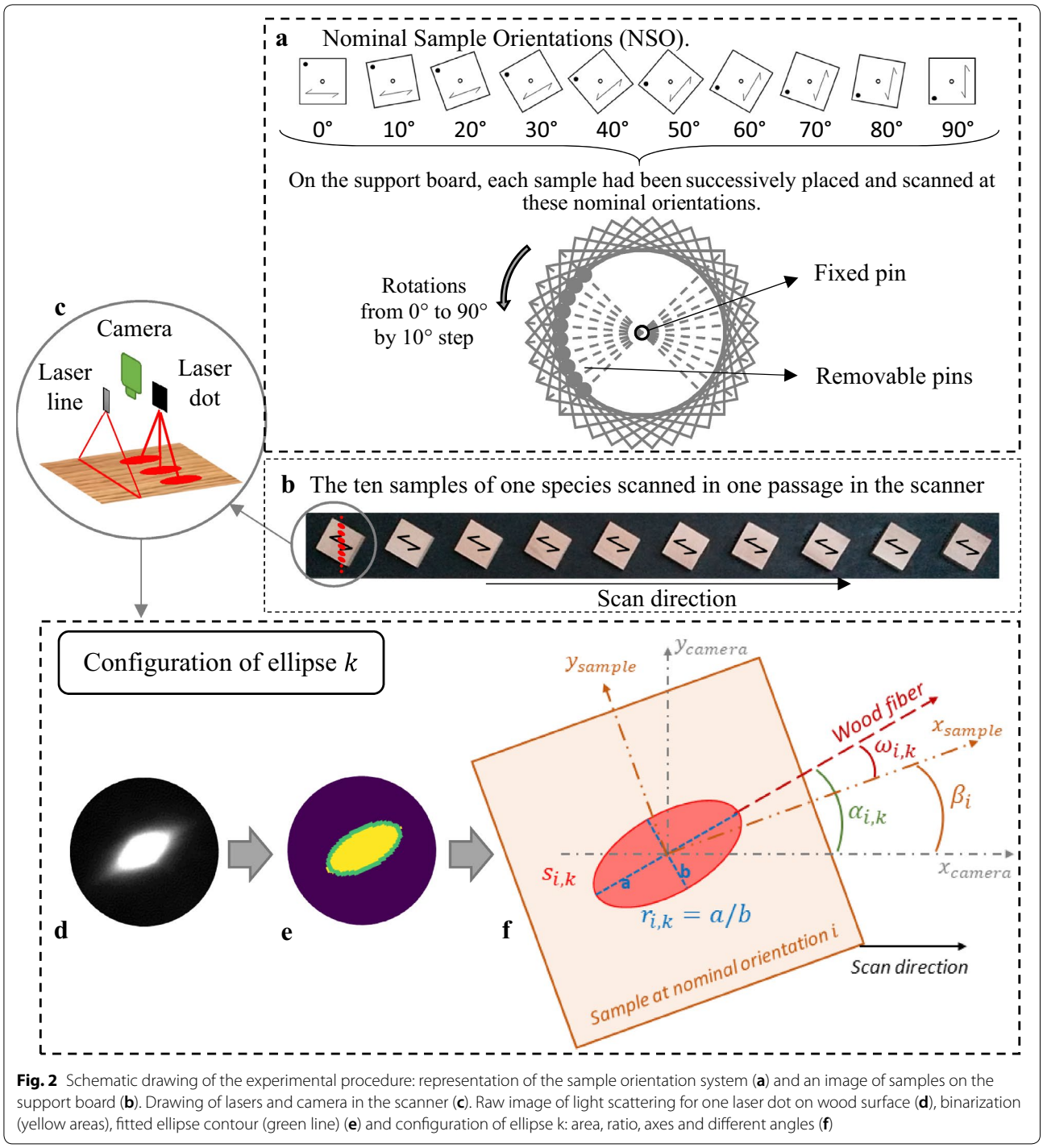

Fig. 2 Schematic drawing of the experimental procedure: representation of the sample orientation system (**a**) and an image of samples on the support board (**b**). Drawing of lasers and camera in the scanner (**c**). Raw image of light scattering for one laser dot on wood surface (**d**), binarization (yellow areas), fitted ellipse contour (green line) (**e**) and configuration of ellipse k: area, ratio, axes and different angles (**f**)

Table 1 Power (mW) of incident laser rays for the two settings of the laser source

	Dot 1	Dot 2	Dot 3	Dot 4	Dot 5	Dot 6	Dot 7	Dot 8	Dot 9	Dot 10	Dot 11	Dot 12	Dot 13	Dot 14	Dot 15
PW (mW)															
Setting 1	5.84	6.28	5.94	7.09	7.39	5.8	7.26	2.36	8.33	6.17	6.75	6.09	6.67	6.02	7.02
Setting 2	3.07	3.36	3.12	3.64	3.81	3.03	3.77	1.21	4.28	3.18	3.51	3.21	3.45	3.19	3.72

between two laser dots. To prevent light spot overlap when fibers were oriented near 90° in relation to the scan direction, laser power was reduced at the setting 2.

Because of a gap observed between the power of the central dot (dot 8 in Table 1) and the others due to laser dividing system, the data coming from this dot were deleted in the following analysis.

In order to detect the scanned piece edges, a laser line was placed next to the laser dot line, oriented perpendicularly to the scan direction (Fig. 2c). The same camera was used to catch the two sets of laser.

Experimental measurements

A set of 10 samples per species was placed on a support board (Fig. 2b) in which 10 holes had been CNC machined in a circular direction from 0° to 90° by 10° step around a central hole. The non-scanned face of each sample had been bored in their middle and in a corner to receive two position pins, so that the scanned surface was free from hole. Each sample was then removable to make possible the sample rotation around the central pin from 0° to 90° by 10° step (Fig. 2a).

The support board was placed on the scanner conveyor along a guide in order to keep the same transversal position for each scan. Therefore, for each nominal orientation, the same laser dots have scanned each sample at the same transversal position.

In order to assess fiber orientation measurement, samples were scanned at 10 orientations defined in the list NSO (nominal sample orientations):

$$\mathrm{NSO} = [0°; 10°; 20°; 30°; 40°; 50°; 60°; 70°; 80°; 90°]$$

The 10 samples were all scanned at the same nominal orientation i in one scan (Fig. 2b). For each sample orientation i in NSO, the real sample orientation—named β_i—was calculated by means of the laser line image, which gave the position of the edges of each sample in camera coordinate system $(x_{\mathrm{camera}}, y_{\mathrm{camera}})$ (Fig. 2f). This was done to correct possible small positioning deviations of samples or of the support board during scanning.

Calculation of ellipse parameters

Laser dots on the wood surface were transformed in quasi-elliptically shaped light spots (Fig. 2d). 8-bit grayscale images of the ellipses were recorded and then binarized (Fig. 2e) with the same threshold of 80, regardless of the laser settings. The contour of the binarized image was then fitted to an ellipse equation in the least square sense (green ellipse in Fig. 2e). From each ellipse, three parameters can be analyzed (Fig. 2f): the ellipse area (s), the ellipse axis ratio (r) (the major axis divided by the minor axis), and the angle (α) between the major axis and the scan direction in camera coordinate system $(x_{\mathrm{camera}}, y_{\mathrm{camera}})$. Axes length of measured ellipses were approximately between 20 (minor axis) and 70 pixels (major axis), that was equivalent to 2.3 and 8 mm, respectively.

The region of interest was 70×70 mm^2 centered on the sample, in order to prevent boundary effect and taking into account the drying shrinkage of oak samples. For each sample at each nominal orientation i, there were, on this region of interest, N measurements of ellipse area, ratio, and fiber orientation named $s_{i,k}$, $r_{i,k}$ and $\alpha_{i,k}$, respectively, with $1 \leq k \leq N$. N was on average equal to 406.

Calculation of sample parameters

Because of fiber orientation variations occurring even on "clear wood" sample, the mean fiber orientation, named A_i of each sample at the orientation i had to be computed: A_i is the average of the N ellipse angles measured on the sample region of interest (Eq. 1). The mean sample ratio R_i and the mean sample area S_i were calculated in a same way from, respectively, $r_{i,k}$ and $s_{i,k}$ (Eqs. 2 and 3):

$$\mathrm{A}_i = \frac{1}{N} * \sum_{k=1}^{N} \alpha_{i,k}, \tag{1}$$

$$R_i = \frac{1}{N} * \sum_{k=1}^{N} r_{i,k}, \tag{2}$$

$$S_i = \frac{1}{N} * \sum_{k=1}^{N} s_{i,k}. \tag{3}$$

The ellipse orientation in sample coordinate system was defined as $\omega_{i,k} = \alpha_{i,k} - \beta_i$, and the mean fiber orientation $\theta_i = \mathrm{A}_i - \beta_i$. Because of the 10° sample rotation between two successive scans, the measurement points were shifted 10° on the sample surface. Therefore, because from one scan to another the orientation measurements were not done on the same fibers, there were some differences between the ten θ_i of a same sample. As a consequence, it was decided to define the reference value of fiber orientation of each sample in sample coordinate system $(x_{\mathrm{sample}}, y_{\mathrm{sample}})$ as the mean of the ten θ_i (Eq. 4). For ratios and areas, the reference value R_{ref}, respectively, S_{ref}, was also defined as the mean of the ten R_i, respectively, S_i (Eqs. 5 and 6):

$$\theta_{\mathrm{ref}} = \frac{1}{10} \sum_{i \in \mathrm{NSO}} (\mathrm{A}_i - \beta_i) \tag{4}$$

$$R_{\mathrm{ref}} = \frac{1}{10} \sum_{i \in \mathrm{NSO}} R_i \tag{5}$$

$$S_{\text{ref}} = \frac{1}{10} \sum_{i \in \text{NSO}} S_i. \tag{6}$$

Measurement error calculation

For a given sample scan, the measurement error δ_i (Eq. 7) is the difference of measured mean fiber orientation in camera coordinate system (A_i) and the theoretical orientation value, which was defined as the addition of the sample reference value (θ_{ref}) and the sample orientation (β_i). In other terms, it is the difference between the mean fiber orientation in the sample coordinate system for the i nominal angle (θ_i) and the mean reference fiber orientation of this sample (θ_{ref}):

$$\delta_i = A_i - (\theta_{\text{ref}} + \beta_i) = \theta_i - \theta_{\text{ref}}. \tag{7}$$

For each species, there were two groups of 5 samples for each orthotropic plane of symmetry (LT or LR), with each sample scanned 10 times between 0° and 90° nominal orientation. Thus, there were for each species and orthotropic plane of symmetry 50 measurements of error. The root mean square of these errors was computed as in Eq. 8:

$$\text{RMSE} = \sqrt{\frac{1}{50} \sum_{j=1}^{5} \sum_{i \in \text{NSO}} \delta_{i,j}^2}, \tag{8}$$

where i is the nominal sample orientation, and j the sample number.

Results

Fiber orientation measurements

Figure 3 shows the mean angles A_i (experimental points) for one typical sample of each species and each orthotropic plane of symmetry. The solid and dashed lines represent the theoretical rotation angle ($\theta_{\text{ref}} + \beta_i$), for LT plane and LR plane, respectively. For oak, the presented results came from the same LT and LR samples at three different states, namely green, dry and sanded.

For wood species scans at 0° sample orientation, fiber orientation was not exactly equal to 0°. Even if a wood piece seems to be straight-grained at a visual appreciation, there are still small fiber deviations.

By rotating by 10° and scanning solid wood samples, mean fiber orientation increased by approximately 10°, as shown in Fig. 3. For all tested wood species and orthotropic planes of symmetry, the evolution of mean measured angles was close to the theoretical values obtained from sample orientation. It is not the case for the HDF sample: the mean measured orientation was between 30° and 50°, whatever the orientation of the sample.

Measurement error

Figure 4 shows the measurement error values (RMSE) per orthotropic plane of symmetry for each species group. The RMSE of HDF samples was 24.2°. For solid wood samples, LT plane RMSE was lower than LR plane RMSE, except for poplar for which they were the same and sweet chestnut for which LT plane RMSE was slightly higher than LR plane RMSE (around 0.1°). For oak, the errors were approximately twice as large on LR plane as on LT plane. Except for oak LR plane samples, for which error reached 3.1°, the measurement error was less than 1.6°. For sweet chestnut, Douglas fir and poplar, error was near 0.9°.

Considering the oak sample states, the lowest RMSE were obtained for dry oak. In comparison, green oak RMSE were, respectively, 0.1° and 0.6° higher for LT and LR planes, and sanded oak RMSE were, respectively, 0.2° and 0.4° higher for LT and LR planes.

Ellipse shape parameters

From one scan to another, the measured points were not exactly at the same positions because of the sample rotation. For each sample, the data from the 10 sample orientations were merged and plotted on data-maps (Fig. 5) with a higher resolution (1×1 mm^2 on interpolated data-maps in Fig. 5d–g). Examples of the data-maps obtained for $\omega_{i,k}$, the ellipse orientations in sample coordinate system, along with the ratios $r_{i,k}$, and areas $s_{i,k}$, are shown in rough maps in Fig. 5c–g respectively, and interpolated (with the nearest neighbor method) maps in Fig. 5d–h, respectively. This is an example of sweet chestnut LT plane sample. The pixel color gives the value of the studied parameter. However, data coming from laser dot 8 being not considered, a lack of rough data was generated in the central part of samples. This had only an impact on the interpolation, all results being based on rough data.

Figure 5b and d shows that almost no fiber was oriented at 0° in sample coordinate system $(x_{\text{camera}}, y_{\text{camera}})$, despite the visually clear wood material. For this sweet chestnut sample, variations between 0° and 12° have been observed.

Figure 6 shows some typical interpolated data-maps of Douglas fir LT plane, sanded oak LT plane and sanded oak LR plane. On the Douglas fir sample, the variations of ratios appeared to be clearly dependent on the initial wood and latewood areas visible in this LT plane (Fig. 6a and c). No clear pattern appeared considering the areas (Fig. 6d). Angle variations were small for the Douglas fir LT plane sample and the oak LT plane sample (Fig. 6b and f), but some great variations were locally observed for angle and ratio interpolated data-maps of oak LR

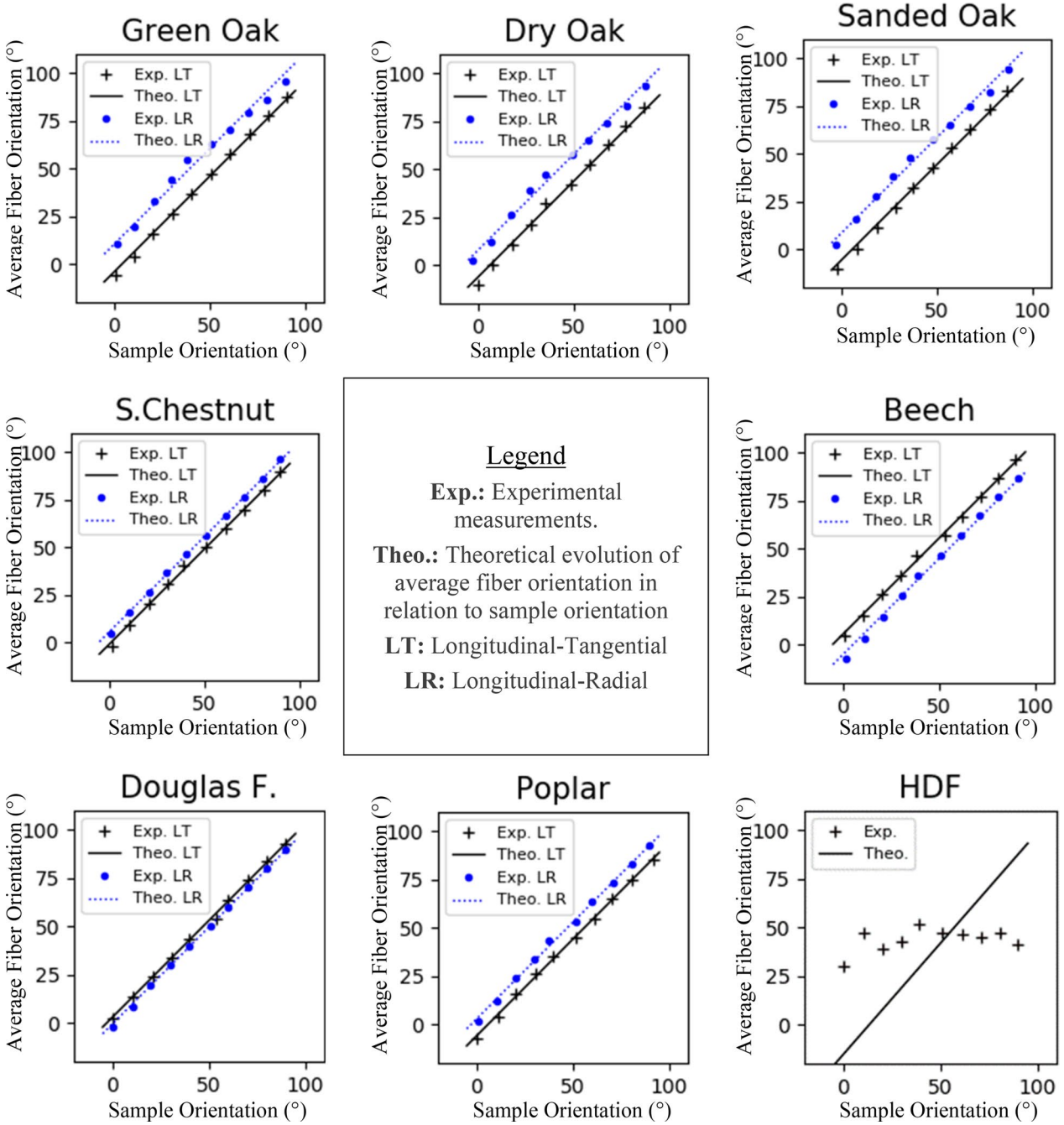

Fig. 3 Results of fiber orientation measurements coming from scans at the ten-sample orientations

plane (Fig. 6j and k). The latter is a result of the big medullary rays, typical of oak (Fig. 6i).

In order to compare visually all the results, data were sorted by species and represented by means of violin plots (Fig. 7). This graph tool allows to display data distribution curves for LT plane on the left side and for LR plane on the right side. The median value for each group is drawn with horizontal black bold line and the 25th and 75 th percentiles are drawn with horizontal black dashed lines. A representative ellipse for each orthotropic plane of symmetry and species has been drawn from reference ratio R_{ref} and area S_{ref} (Fig. 7b). This representation gives an overview of the laser light spot on samples during the measurement. For HDF, the

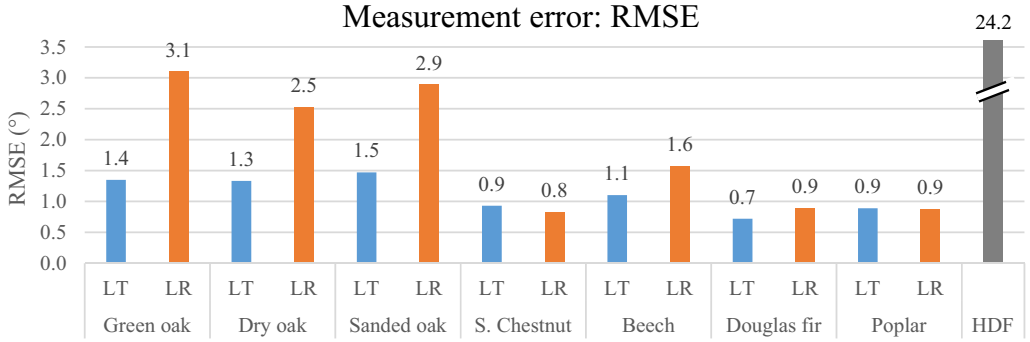

Fig. 4 Measurement error: RMSE sorted by species and orthotropic planes of symmetry

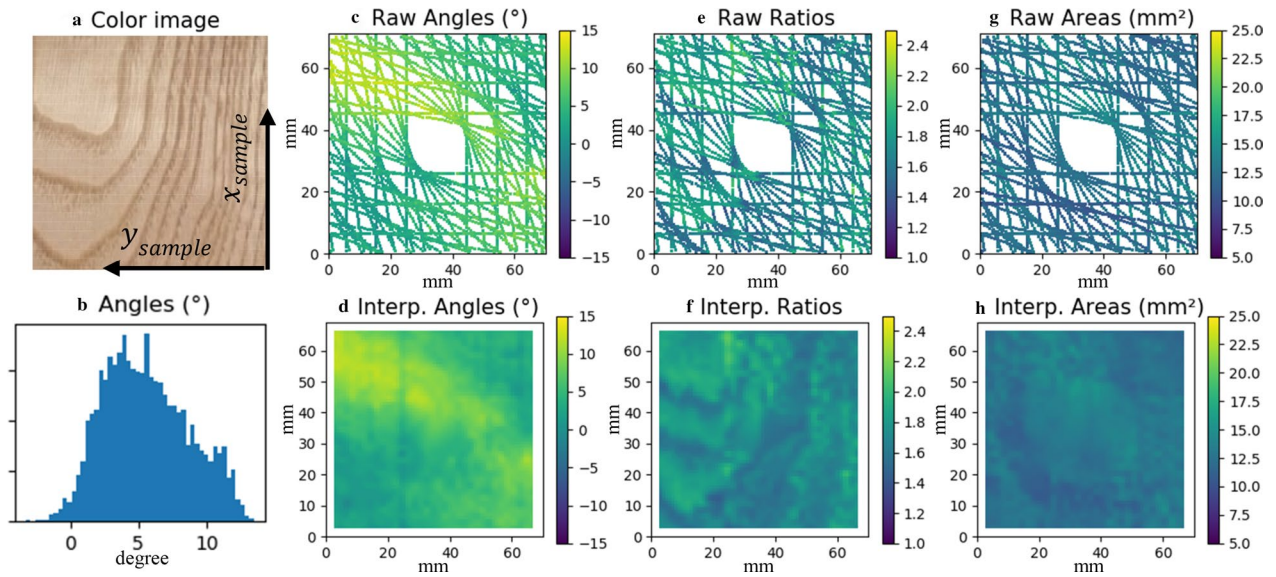

Fig. 5 Data from sample: color image (**a**), histogram of raw angles (**b**) and data-maps of sweet chestnut LT plane sample: raw angles $\omega_{i,k}$ (**c**) and interpolated (**d**) angles $\omega_{i,k}$, raw ratios $r_{i,k}$ (**e**) and interpolated (**f**) ratios $r_{i,k}$, raw areas $s_{i,k}$ (**g**) and interpolated (**h**) areas $s_{i,k}$. In data-maps, the color level of pixels shows the value of relevant parameter

light spot was visually circular, while for poplar, e.g., it was a long and narrow ellipse. There was no clear ellipse size difference between green oak and dry and sanded oak because the green oak samples were scanned at lower laser power in order to not have too big ellipses. Poplar ellipses would have been also too big if the same power as the other samples was used.

Ratio analysis enables to describe and quantify ellipse geometry and shows if light spots are more circular or elliptic. The more light spots are circular, the more fiber orientation measurement is difficult. HDF ratios were very low, 95% of them staying below 1.12. Laser light spots on this material were almost circular, which means light was not scattering in a specific direction. The wood species scanned here did not reach such low values, except oak in LR plane: for green oak, 8.5% of the ratios were lower than HDF 95th percentile, 9.4% for dry oak and 8% for sanded oak.

For all species, ellipse ratios were always lower for LR plane in comparison to LT plane. A similar behavior could be observed regarding ellipse areas, but with a lower order of magnitude, and excepting poplar for which ellipse areas were higher for LR plane than LT plane. Considering the samples scanned at the setting 1, the average of HDF ellipse areas was the smallest with 6.5 mm^2, while the average of ellipse areas was near 11 mm^2 on dry oak and sanded oak, 14 mm^2 on beech, 13.5 mm^2 on sweet chestnut and 17.5 mm^2 on Douglas fir. Considering the samples scanned at the setting 2,

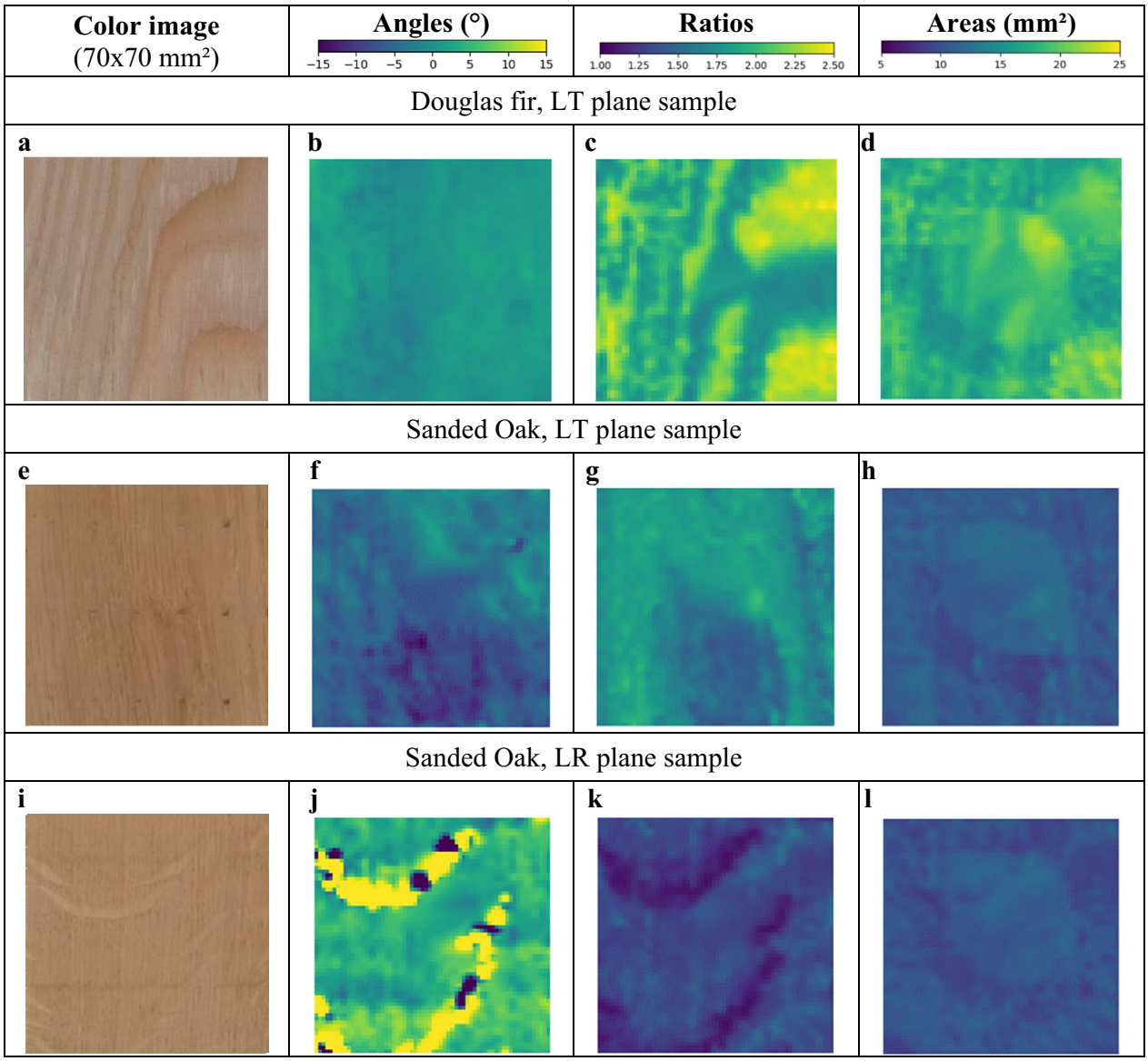

Fig. 6 Data in the form of maps: color image and interpolated data-maps (70 × 70 mm^2) of angles, ratios and areas for LT plane sample of Douglas Fir (**a**–**d**), LT plane sample of sanded oak (**e**–**h**) and LR plane sample of sanded oak (**i**–**l**)

the average of green oak ellipse areas was near 10 mm^2 while on poplar, it was near 12 mm^2.

Poplar presented the highest ratios and that despite the reduced laser power, especially for LT plane (median ratio equal to 2.4). The second higher median ratios were that of Douglas fir, but with a very large scattering of values. Indeed, two different distributions are visible for LT plane. Oak was the species with the smallest ratios. Globally, ratios were similar between the three oak sample states and that despite the reduced laser power for green oak. The difference of surface machining quality did not introduce changes of ellipse ratio, and this was especially noticeable for dry oak and sanded oak which were scanned at the same laser power.

Relationship between ellipse ratios and RMSE of angle measurements

Figure 8 shows the relationship between the reference value of ellipse ratios R_{ref} and RMSE of angle measurements. Bolt points in Fig. 8 represent data of sample groups previously described. Triangles represent data coming from each of the three states of LR plane oak for

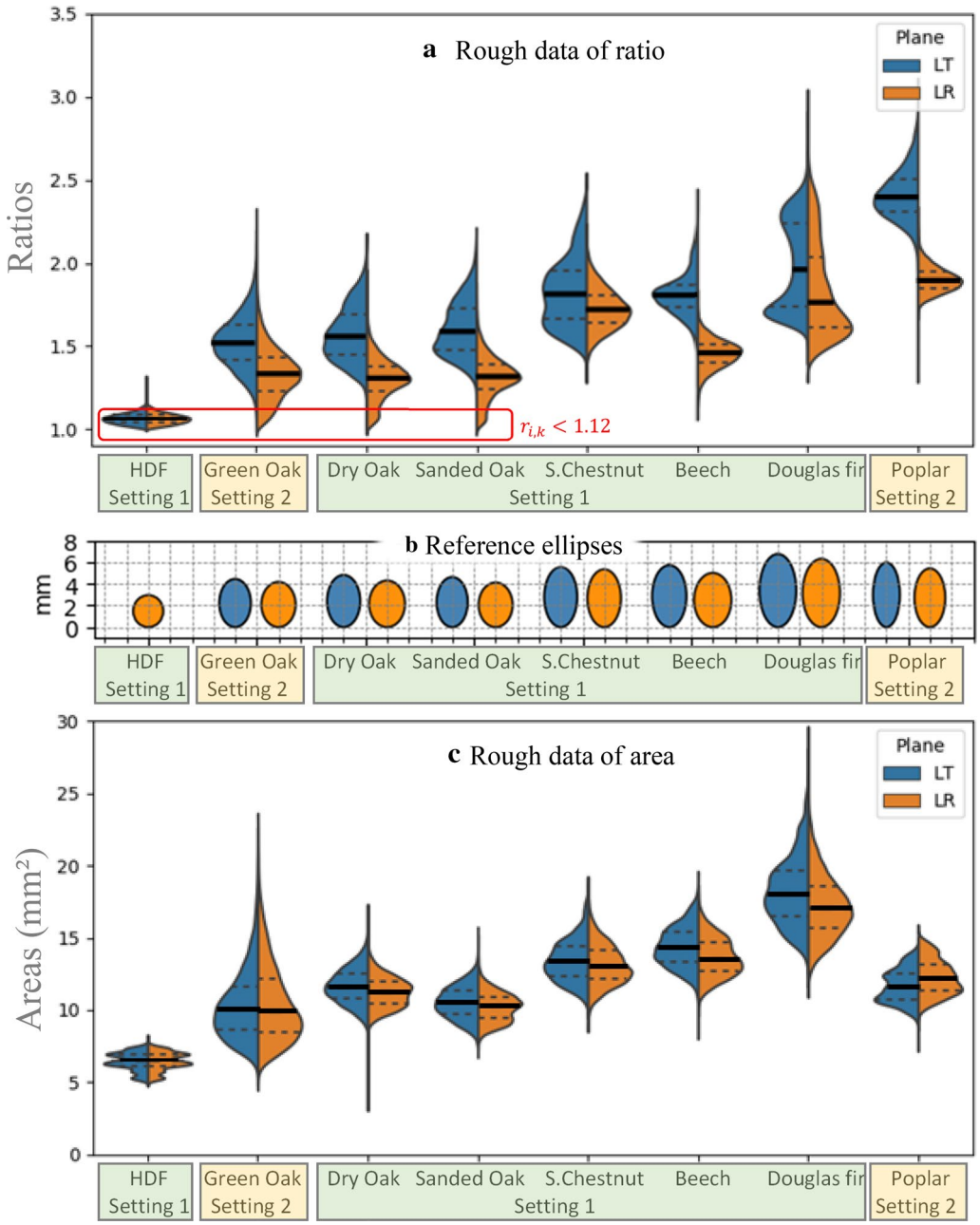

Fig. 7 Ellipse comparison between species: Ellipse RATIO by species displayed by violin plots (**a**): data from LT plane in blue, data from LR plane in orange (colors not relevant for HDF), medians (bolt lines) and 25th and 75th percentiles (dashed lines). Reference ellipse drawing from R_{ref} and S_{ref}, sorted as (**a**, **b**). Ellipse AREA data represented by species by means of violin plots, sorted as (**a**, **c**)

which measurement errors were calculated with only ellipse ratios $r_{i,k}$ higher than 1.12, threshold value equal to the 95th percentile of HDF ellipse ratio.

The measurement error clearly depended on the ratio: RMSE were higher for lower ratios. For green oak, dry oak and sanded oak LR plane, measurement error was lower when lower ratios were removed (GO2-LR, DO2-LR and SO2-LR). Reference ratios higher than 1.7 made it possible to have errors lower than 1° or very close. There was no improvement in the RMSE for ratios higher than 1.7.

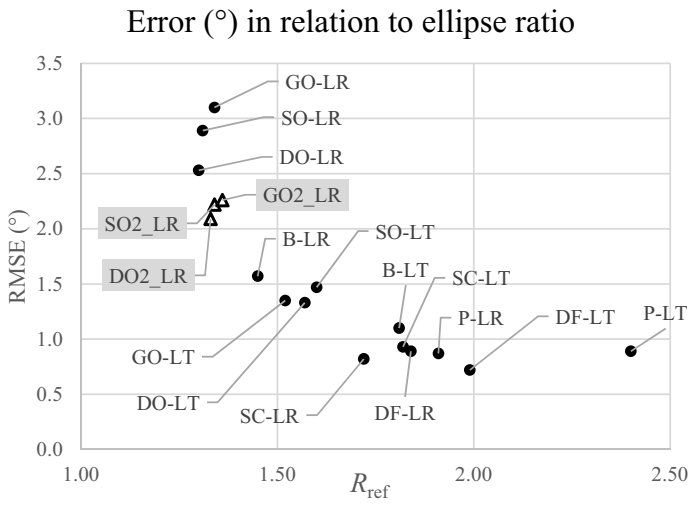

Legend	
GO-LT	Green Oak LT
GO-LR	Green Oak LR
DO-LT	Dry Oak LT
DO-LR	Dry Oak LR
SO-LT	Sanded Oak LT
SO-LR	Sanded Oak LR
SC-LT	S. Chestnut LT
SC-LR	S. Chestnut LR
B-LT	Beech LT
B-LR	Beech LR
DF-LT	Douglas fir LT
DF-LR	Douglas fir LR
P-LT	Poplar LT
P-LR	Poplar LR
GO2-LR	Green Oak LR**
DO2-LR	Dry Oak LR**
SO2-LR	Sanded Oak LR**

** Results for $r_{i,k}$>1.12

Fig. 8 Correlation between measurement error and ellipse ratios: RMSE as a function of mean ratio R_{ref} (only solid wood samples)

Discussion

For all the solid wood samples, the measured angles were well correlated to sample rotations (low RMSE), while as expected for HDF, there was not such a correlation (high RMSE). This shows it is possible to make a reliable measurement of the fiber orientation on all the species tested. This latter result is different from that of [13], who did not find satisfactory results for oak (*Quercus spp.* L.). This discrepancy should come from the different material setups and method used.

Although HDF-measured angles were not correlated with sample rotation (Fig. 3), thus there was no specific grain direction, the significant size of ellipse areas showed nevertheless a light scattering effect, but in all directions. Despite quasi-circular light spots, the applied binarization and fit ellipse method was able to find an ellipse angle, constant even when rotating the sample, which can be explained by the imperfect roundness of the incident laser dots. Thus, it was the initial orientation of the laser dots which was actually measured by projecting them on an isotropic surface like HDF.

Influence of parenchyma

According to the ellipse analysis for LT and LR planes (Fig. 7), ratio appears as the more sensible parameter, in particular to the orthotropic plane of symmetry. As Fig. 8 shows, there was a genuine correlation between angle measurement error and ratio. Several phenomena can explain that.

Ellipses with low ratios, close to those obtained on HDF, were numerous on LR plane of oak samples, which is in accordance with the fact that these solid wood samples presented the highest errors of fiber orientation measurements. According to the observation of the color images and the data-maps of these samples, lower ratios were located in specific areas with large medullary rays, a distinctive characteristic of oak (Fig. 6i, j). This could be explained by the fact that rays are parenchyma cells oriented in the radial direction, but not in longitudinal direction as fibers [14]. Thus, they may scatter the laser light in perpendicular direction to wood fibers, or scatter less light. Anyhow, what appears clearly is that they locally disturb the fiber orientation measurement, which increases the RMSE. For these samples, if ratios under the HDF 95th percentile value were removed, RMSE would decrease to 2.3° for green oak, to 2.1° for dry oak and to 2.2° for sanded oak, instead of 3.1°, 2.5° and 2.9°, respectively (Fig. 8). It is as if big medullary rays have been removed. In LT plane, medullary rays have no such impact because their "longitudinal" direction does not appear in this plane. The errors obtained on sweet chestnut, wood having the same anatomical structure as oak but without any visible medullary rays, confirm this interpretation of the result. Moreover, beech was the species with the second lowest ratios ($R_{ref}=1.45$) and the second highest RMSE (1.6°), which confirms also this interpretation, beech having on LR plane the most visible medullary rays after oak.

The other species have also parenchyma cells in LR plane, but they are less visible than oak massive rays. In the point of view of light scattering, these cells, oriented across fiber direction, could contribute to increase slightly light scattering in the radial direction and then to interfere and decrease it slightly in the longitudinal direction. This would be a first explanation of the higher minor axis and lower major axis visible in reference ellipses in

Fig. 7b, hence the smaller ratios. A second possible explanation could be an orthotropic behavior of light scattering due to radial growth, as it is the case for mechanical properties. These two assumptions could explain why on beech, poplar and oak, the ratio differences between LT and LR plane were very pronounced.

Influence of annual growth

Figure 7 shows some other anatomic particularities. On Douglas fir samples, the two visible ratio populations clearly came from the difference of light scattering on early wood and late wood. Ratios seem to be bigger for late wood than for early wood (Fig. 6a and c). This phenomenon was more visible on LT samples because late wood, for which ratios were higher, was present in bigger areas than for LR plane samples. Sweet chestnut LT samples presented also similar differences of ratio populations, for a similar reason with ellipse ratios smaller when laser beam was on initial porous area. Nevertheless, ellipse ratios on these two species were high enough to have a low measurement error.

Comparison between oak sample states

About the ellipse size comparison between the different states of oak samples, the influence of surface MC was not clearly visible because of the use of reduced laser power for green oak sample scans. There was no significant difference between dry and sanded oak. Regarding the fiber orientation measurement, and considering the settings used in this study, moisture content and roughness of scanned oak surfaces did not significantly affect the fiber orientation measurement. Indeed, when taking into account sample surfaces free from big medullary rays, RMSE differences between green and dry oak were only 0.1° and 0.2° for LT and LR planes, respectively, and the RMSE differences between dry rough sawn oak and dry sanded oak were only 0.2° for LT and LR planes. These similar RMSEs did not highlight any influence of MC and surface machining on oak fiber orientation measurement. In the literature, authors like [9] and [5] have yet showed that a better surface machining generated better fiber orientation measurements by laser light scattering. However, it was observed in species other than oak, i.e., Douglas fir for the first one and sugi and Japanese beech for the second one and using different material setups. That may explain these different results in this study.

Conclusion

With the sample rotation method used in this paper, the error of fiber orientation measurement on clear wood have been successfully calculated for different European hardwoods and one softwood species. For most of them, the RMSE were higher on LR plane compared to LT plane, which highlights the influence of wood anatomy on the laser light scattering (often called "tracheid effect" in the literature). The reason of this behavior, which seemed to be unreported in the literature until now, would be the more circular shapes of ellipse in LR plane because of the presence of parenchyma cells.

Moreover, ellipse shape analysis showed that the measurement error was correlated to ellipse axis ratio, ellipses with smaller ratio giving higher errors. It seems possible to measure grain angle with ellipse even with rather small ratios (near 1.35) with an acceptable error (near 3°). For ellipse with ratio higher than 1.5, measurements with an error less than 1.5° are possible.

In a general manner, RMSE was below 1.6°, apart for oak LR plane, whatever its states (green, dry or sanded). This was due to the fact that measurement were highly affected by medullary rays, leading to a RMSE of 3.1°. Nevertheless, these error levels seem compatible with efficient measurements used for strength grading and/or knot detection. As a result, fiber orientation measurement was successfully performed on all the tested species.

Abbreviations

ANRT: Association Nationale de la Recherche et de la Technologie; B: Beech; CNC: Computer numerical control; CIFRE: Conventions Industrielles de Formation par la REcherche; DF: Douglas fir; DO: Dry oak; Fig: Figure; FPS: Fiber saturation point; GO: Green oak; HDF: High-density fiberboard; Interp.: Interpolated; LR: Longitudinal–radial; LT: Longitudinal–tangential; MC: Moisture content; NIR: Near infra-red; NSO: Nominal sample orientation; P: Poplar; PW: Power; RMSE: Root mean square error; SC: Sweet chestnut; SO: Sanded oak.

Acknowledgements

The authors thank Jean-Claude Butaud from Arts et Métiers Cluny for his technical support during the production of data and his review. They thank their financial collaborators, especially Ducerf Groupe who followed this study closely. They also thank Rémy Marchal from Arts et Métiers Cluny for his review.

Authors' contributions

BB: production and treatment of the data, data analysis, writing. GP: data analysis, writing, supervision. RC: main supervision, interpretations, review. JV: treatment and analysis of the data, review.

Funding

This study was funded by Ducerf Groupe, the Association Nationale de la Recherche et de la Technologie (ANRT) (CIFRE convention N°2018/0987) and the regional council of Bourgogne Franche-Comté.

Availability of data and materials

The datasets used and/or analyzed during the current study are available from the corresponding author on reasonable request.

Competing interests
The authors declare that they have no conflict of interest.

Received: 29 July 2020 Accepted: 16 October 2020
Published online: 21 October 2020

References

1. Nyström J (2003) Automatic measurement of fiber orientation in softwoods by using the tracheid effect. Comp Electron Agric 41:91–99
2. Simonaho SP, Palviainen J, Tolonen Y, Silvennoinen R (2004) Determination of wood grain direction from laser light scattering pattern. Opt Lasers Eng 41:95–103
3. Soest J, Matthews P, Wilson B (1993) A simple optical scanner for grain defects. Proceedings of Fifth International Conference on Scanning Technology and Process Control for the Wood Products Industry, Atlanta
4. Zhou J, Shen J (2003) Ellipse detection and phase demodulation for wood grain orientation measurement based on the tracheid effect. Opt Lasers Eng 39:73–89
5. Hu C, Tanaka C, Ohtani T (2004) On-line determination of the grain angle using ellipse analysis of the laser light scattering pattern image. J Wood Sci 50:321–326
6. Briggert A, Hu M, Olsson A, Oscarsson J (2018) Tracheid effect scanning and evaluation of in-plane and out-of-plane fiber direction in Norway spruce timber. Wood Fiber Sci 50:411–429
7. Olsson A, Oscarsson J, Serrano E, Källsner B, Johansson M, Enquist B (2013) Prediction of timber bending strength and in-member cross-sectional stiffness variation on the basis of local wood fibre orientation. Eur J Wood Wood Products 71:319–333
8. Viguier J, Jehl A, Collet R, Bleron L, Meriaudeau F (2015) Improving strength grading of timber by grain angle measurement and mechanical modeling. Wood Mat Sci Eng 10:145–156
9. Daval V, Pot G, Belkacemi M, Meriaudeau F, Collet R (2015) Automatic measurement of wood fiber orientation and knot detection using an optical system based on heating conduction. Opt Express 23(26):33529–33539
10. Jolma I, Mäkynen A (2008) The detection of knots in wood materials using the tracheid effect. Proc SPIE doi 10(1117/12):803924
11. Kienle A, D'Andrea C, Foschum F, Taroni P, Pifferi A (2008) Light propagation in dry and wet softwood. Opt Express 16:9895–9906
12. Purba CYC, Viguier J, Denaud L, Marcon B (2020) Contactless moisture content measurement on green veneer based on laser light scattering patterns. Wood Sci Technol. https://doi.org/10.1007/s00226-020-01187-0
13. Schlotzhauer P, Wilhelms F, Lux C, Bollmus S (2018) Comparison of three systems for automatic grain angle determination on european hardwood for construction use. Eur J Wood Wood Prod 76:911–923
14. Carlquist S (2001) Comparative wood anatomy: systematic, ecological, and evolutionary aspects of dicotyledon wood springer series in wood science. Berlin Heidelberg: Springer-Verlag. https://doi.org/10.1007/978-3-662-04578-7

Publisher's Note